DALTON
FULL PAPER

Metal-centred *versus* ligand-centred luminescence quenching of a macrocyclic copper(II) complex †

Paul V. Bernhardt,* Bernadine M. Flanagan and Mark J. Riley

Department of Chemistry, University of Queensland, Brisbane 4072, Australia

Received 12th April 1999, Accepted 1st September 1999

The new macrocyclic ligand *trans*-6-(9-anthracenylmethylamino)-6,13-dimethyl-1,4,8,11-tetraazacyclotetradecan-13-amine has been synthesized and characterised as its copper(II) complex and the crystal structure of this complex has been determined. Fluorescence of the anthracenyl group of the macrocycle is quenched in its free base form and when complexed with Cu^{II}. Fluorescence returns when Lewis acids such as H^+ and Zn^{II} are added to solutions of the ligand, indicating that photoinduced electron transfer from the amine lone pairs is responsible for fluorescence quenching in the free base form. By contrast, fluorescence of the complex is quenched by intramolecular electronic energy transfer.

The modulation of luminescence of a system in the presence or absence of other molecules forms the basis of fluorescent sensing. One of the most studied fluorophores is anthracene and its derivatives. It has been shown that the strong blue fluorescence of anthracene may be quenched by a variety of mechanisms including photoinduced electron transfer (PET) and electronic energy transfer (EET). The analog 9-aminomethylanthracene has been extensively studied as a fluorescent pH sensor.[1] In its free base form the amine lone pair undergoes a PET reaction with the aromatic ring system and the anthracenyl fluorophore is reductively quenched. In acidic solution the protonated ammonium group cannot be oxidised, electron transfer from the amine lone pair is deactivated and fluorescence returns. Several variations on this theme are known that incorporate metal ions[2–4] or boronic esters[5,6] as Lewis acids (instead of H^+), which deactivate the amine lone pair and thus prevent fluorescence quenching *via* PET.

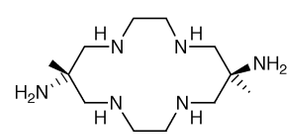

L^1

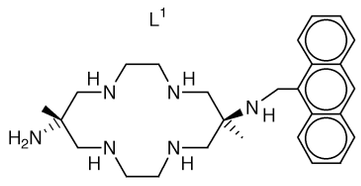

L^2

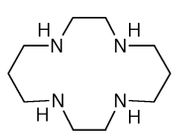

L^3

In competition with EET and luminescence, PET from the metal or the amine is possible in systems where both a redox active metal and a free 9-aminomethylanthracene group are present. However, the amine proximate to the anthracene group has invariably been involved in metal ion binding,[2,7–9] so discrimination between the two PET pathways has not been possible. In this work, we have prepared and characterised the new pendant armed macrocycle *trans*-6-(9-anthracenylmethylamino)-6,13-dimethyl-1,4,8,11-tetraazacyclotetradecan-13-amine as its copper(II) complex. The preferred pseudo square planar co-ordination geometry of Cu^{II} disfavors co-ordination by the pendant amines in solution, leaving the amine lone pair proximate to the anthracene group free to react. In competition with this process, the metal centre may undergo a photoinduced reduction or oxidation or act as an energy sensitiser for the luminophore. In this work, we will show how each of these processes compete, and how one can modulate the luminescence behavior of the macrocyclic fluorophore in the presence of a variety of Lewis acids.

Experimental

Syntheses

The parent ligand *trans*-6,13-dimethyl-1,4,8,11-tetraazacyclotetradecane-6,13-diamine hexahydrochloride ($L^1 \cdot 6HCl$) was prepared as previously described.[10] 9-Anthraldehyde was synthesized according to a literature procedure.[11]

***trans*-(6-(9-Anthracenylmethylamino)-6,13-dimethyl-1,4,8,11-tetraazacyclotetradecan-13-amine)copper(II) perchlorate ($[CuL^2][ClO_4]_2$).** A solution of $L^1 \cdot 6HCl$ (6.0 g) and triethylamine (12 cm^3) in ethanol (600 cm^3) was prepared to give a clear solution of the free base. To this was added 9-anthraldehyde (2.07 g) and the mixture stirred at 25 °C for 16 h. A fine yellow precipitate formed during the reaction, $NaBH_4$ (5.0 g) was added in portions and the mixture refluxed for 1 h. The solvent was removed by rotary evaporation and the residue suspended in water. The yellow precipitate was collected by filtration and dried in a vacuum desiccator. Purification of the ligand L^2 was achieved through complexation as described below.

The above yellow solid (3.0 g) was mixed with copper(II) acetate hydrate (1.33 g) in a mixture of MeCN (200 cm^3) and water (100 cm^3) to give an immediate purple solution. After 15 min of stirring, MeCN was removed on a rotary evaporator. A brown precipitate formed, which was removed by filtration and discarded. The purple filtrate was charged onto a Sephadex C-25 cation exchange column (Na^+ form). The eluent was 2 mol dm^{-3} sodium acetate. Free Cu^{2+} eluted first, followed by traces of $[CuL^1]^{2+}$. The desired product eluted last, well after any other

† *Supplementary data available*: rotatable 3-D crystal structure diagram in CHIME format. See http://www.rsc.org/suppdata/dt/1999/3579/

bands. Addition of 1 mol dm^{-3} $NaClO_4$ solution (200 cm^3) afforded immediate and quantitative precipitation of the complex (0.59 g). This solid was suspended in MeCN (*ca.* 10 cm^3) and filtered to remove any NaOAc that had co-crystallised. Vapour diffusion of diethyl ether into the filtrate afforded purple crystals of the complex suitable for X-ray work. All spectroscopic and electrochemical measurements were performed with these crystals. Electronic spectrum (MeCN): λ_{max} 498 (ε 125), 386 (7720), 366 (8480), 348 (5550), 332 (2820) and 316 nm (ε 1390 dm^3 mol^{-1} cm^{-1}).

***trans*-6-(9-Anthracenylmethylamino)-6,13-dimethyl-1,4,8,11-tetraazacyclotetradecan-13-amine).** A solution of $[CuL^2][ClO_4]_2$ (0.1 g) in water (75 cm^3) was demetallated by addition of excess of $Na_2S{\cdot}9H_2O$ (1 g) to give a precipitate of CuS, which was complete after stirring at room temperature for 15 min. The mixture was extracted with CH_2Cl_2 (3×50 cm^3), and the extracts, containing the free base L^2, were dried over Na_2SO_4. The mixture was filtered and evaporated to dryness. NMR: ^1H ($CDCl_3$) δ 1.06 (s, 3 H, CH_3), 1.40 (s, 3 H, CH_3); 2.18 (s br, 7 H, NH); 2.5–3.0 (m, 16 H, CH_2), 4.72 (s, 2 H, CH_2NH), 7.5 (m, 4 H), 8.0 (d, 2 H), 8.38 (s, 1 H) and 8.44 (d, 2 H); ^{13}C ($CDCl_3$) δ 23.1, 27.6, 38.1, 48.6, 48.9, 51.3, 55.7, 57.8, 60.7, 124.4, 124.9, 125.9, 127.0, 129.1, 130.4, 131.6 and 132.1.

Physical methods

Nuclear magnetic resonance spectra were measured at 200 (^1H) and 50.3 MHz (^{13}C) on a Bruker AC200 spectrometer referenced with tetramethylsilane. Electrochemical measurements were carried out with a BAS 100B/W potentiostat, using a glassy carbon working, platinum Pt auxiliary and a gold reference electrode. Potentials were referenced with the ferrocene–ferrocenium couple (+0.34 V *vs.* NHE). All electrochemical solutions contained *ca.* 5 mmol dm^{-3} of analyte and 0.1 mol dm^{-3} n-Bu_4NClO_4 dissolved in MeCN, and were purged with nitrogen before measurement. Electronic spectra were measured with a Perkin-Elmer Lambda 12 UV-Vis spectrometer. Luminescence measurements were employed a Perkin-Elmer LS50B luminescence spectrometer using 10^{-4} mol dm^{-3} solutions in MeCN. Front face excitation was employed to compare relative intensities of the emission from solutions and glasses. Infrared spectra of compounds dispersed in KBr discs were measured using a Perkin-Elmer 1600 Series FT-IR spectrometer. Aqueous pulse radiolysis measurements were performed with a 20 MeV linear accelerator at the Australian Radiation Laboratories, Melbourne. Reductions were effected by radiolytically generated aquated electrons (e_{aq}^-) in the presence of deoxygenated aqueous 0.1 mol dm^{-3} t-BuOH which quenched $^{\bullet}OH$ and $^{\bullet}H$ radicals also produced by the pulse, eqns. (1a) and (1b). Oxidations were achieved with the $^{\bullet}OH$

$$^{\bullet}OH + t\text{-BuOH} \longrightarrow H_2O + {}^{\bullet}H_2CC(CH_3)_2OH \quad (1a)$$

$$^{\bullet}H + t\text{-BuOH} \longrightarrow H_2 + {}^{\bullet}H_2CC(CH_3)_2OH \quad (1b)$$

radical by saturating each solution with N_2O, which converted all e_{aq}^- into $^{\bullet}OH$ radicals thus producing an extra equivalent of oxidant, eqn. (2). Dosimetry was performed with N_2O purged

$$e_{aq}^- + N_2O + H_2O \longrightarrow {}^{\bullet}OH + N_2 + OH^- \quad (2)$$

0.02 mol dm^{-3} KSCN solutions, which generated the $(SCN)_2^{-\bullet}$ radical ($\varepsilon_{480\,nm}$ 7600 dm^3 mol^{-1} cm^{-1}). Typical concentrations in their respective reduction and oxidation experiments were 2×10^{-5} (e_{aq}^-) and 4×10^{-5} mol dm^{-3} ($^{\bullet}OH$). In order to generate pseudo first order formation of all radiolytically generated products, the concentration of each copper(II) complex was always in excess of 5×10^{-4} mol dm^{-3}. Spectra were determined point-by-point at 5 nm (or in some case 2.5 nm) intervals by monitoring the changes in absorbance relative to the spectrum of the starting material.

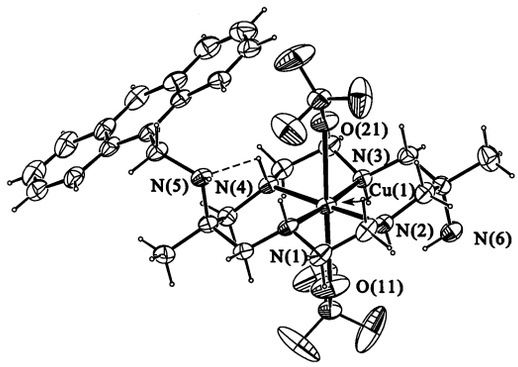

Fig. 1 Drawing of the complex $[CuL^2][ClO_4]_2$. Selected bond lengths (A): Cu(1)–N(1) 2.013(4); Cu(1)–N(2) 2.014(4); Cu(1)–N(3) 2.011(4); Cu(1)–N(4) 1.999(4); Cu(1)–O(11) 2.474(5); Cu(1)–O(21) 2.618(4); C–N 1.46–1.49; C–C (aliphatic) 1.49–1.54; C–C (aromatic) 1.32–1.43.

Molecular mechanics calculations were performed with MOMECPC[12] using a published force field.[13] The anthracene group was modeled with identical C–C bonding parameters. This approximation was acceptable for the present study as the overall steric bulk of the conformationally rigid anthracene group is of primary concern to us rather than internal bond length and angle variations. Perchlorate anions were modelled as ideal tetrahedra: $k_{(Cl-O)}$ 6.5 mdyn $Å^{-1}$, r_o 1.40 Å and k_θ 0.45 mdyn Å rad^{-2}.

Crystal structure analysis

Cell constants were determined by a least-squares fit to the setting parameters of 25 independent reflections measured on an Enraf-Nonius CAD4 four circle diffractometer employing graphite monochromated Mo-Kα radiation and operating in the ω–2θ scan mode. Data reduction and empirical absorption corrections (ψ scans) were applied with the XTAL package.[14] The structure was solved by heavy atom methods with SHELXS 86[15] and refined by full-matrix least-squares analysis with SHELXL 93.[16] Non-H atoms were refined with anisotropic thermal parameters, whereas H atoms were included at estimated positions. The atomic nomenclature is defined in Fig. 1 drawn with the program PLATON.[17]

Crystal data. $[CuL^2][ClO_4]_2$, $C_{12}H_{30}Cl_3CoN_6O_{12}$, $M = 615.7$, triclinic, space group $P\bar{1}$, $a = 8.529(1)$, $b = 9.123(1)$, $c = 21.298(3)$ Å, $\alpha = 87.46(1)$, $\beta = 86.75(1)$, $\gamma = 66.53(1)°$, $U = 1517.2(3)$ $Å^3$, D_c ($Z = 4$) = 1.557 g cm^{-3}, μ(Mo-Kα) = 9.56 cm^{-1}, $T = 293$ K, $N = 5713$, $N_o = 3024$ [$|F_o| > 2\sigma(|F_o|)$, $2 < \theta < 25°$]. Final $R1 = 0.0568$, $wR2 = 0.1426$.

CCDC reference number 186/1637.

See http://www.rsc.org/suppdata/dt/1999/3579/ for crystallographic files in .cif format.

Results

Syntheses and structure

The condensation of 9-anthraldehyde with the pendent amino group of L^1 appeared to be regioselective, and no evidence of reaction at the secondary amines or multiple substitution was found. Purification of the ligand was most easily achieved by complexation, which allowed ready separation from non-ligating by-products such as 9-hydroxymethylanthracene. This led to isolation and crystallisation of the copper(II) complex $[CuL^2][ClO_4]_2$. The crystal structure analysis finds the complex cation on a general site with perchlorate ligands bound axially perpendicular to the macrocyclic plane. A view of the complex is shown in Fig. 1. The Cu–N bond lengths (≈2.01 Å) are consistent with other copper(II) analogues.[18] The configuration of

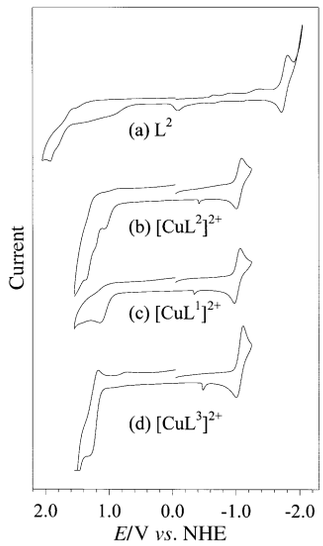

Fig. 2 Cyclic voltammograms of (a) L^2, (b) $[CuL^2]^{2+}$, (c) $[CuL^1]^{2+}$ and (d) $[CuL^3]^{2+}$. Scan rate 100 mV s^{-1} (see Experimental section for more details).

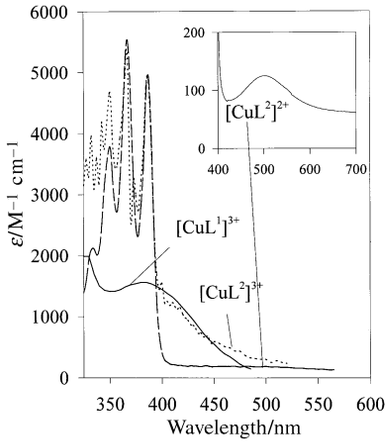

Fig. 3 Aqueous electronic absorption spectra of $[CuL^2]^{2+}$ (----), $[CuL^2]^{3+}$ (····) and $[CuL^1]^{3+}$ (——) where the tripositive ions were generated by pulse radiolytic oxidation of their parent copper(II) complexes. Inset: amplification of visible maximum of $[CuL^2]^{2+}$.

the secondary amines is *RSSR* (*trans*-III) and the two pendant amines adopt axial (α) dispositions with respect to the six-membered chelate rings to which they are attached. The position of the anthracenyl fragment is to one side of the macrocyclic plane and the distance between the centre of the aromatic system and the metal is 6.07 Å. An intramolecular hydrogen-bonding interaction between the free secondary amine and an adjacent co-ordinated secondary amine H atom (N(5)···H–N(4) 2.342(6) Å has a significant bearing on the orientation of the anthracenyl fragment with respect to the macrocycle. There are also several intermolecular amine hydrogen-bonding interactions with perchlorate O atoms and N(6).

Redox chemistry

Cyclic voltammetry of the "free" ligand L^2 yielded anthracene-based redox processes in both the oxidative and reductive sweeps. A reversible L^2–$(L^2)^-$ couple was identified at −1.77 V *vs*. NHE (Fig. 2(a)), and corresponds to reduction of the anthracenyl group to its radical anion. This redox potential is anodically shifted relative to 9-methylanthracene (−1.87 V *vs*. NHE) measured under the same conditions. Irreversible oxidation waves were found at *ca.* +1.3 (broad) and +1.9 V *vs*. NHE. By comparison, the parent ligand L^1 gives only a single irreversible wave at +1.2 V *vs*. NHE. Clearly the less positive responses are due to amine oxidations, while the more positive response in the voltammogram of L^2 may be assigned to oxidation of the anthracenyl group, which is comparable with the oxidation potential of anthracene (+1.56 V *vs*. NHE).

Cyclic voltammetry of $[CuL^2]^{2+}$ in MeCN identified both metal- and ligand-centred responses. A totally reversible $Cu^{II/I}$ couple at −1.05 V *vs* NHE was identified when the potential was reversed at −1.3 V (Fig. 2(b)). Almost identical behaviour was found for the closely related $[CuL^1]^{2+}$ and $[CuL^3]^{2+}$ complexes (Fig. 2(c) and 2(d)). When a switching potential of −2.2 V *vs*. NHE was employed the $Cu^{II/I}$ wave of $[CuL^2]^{2+}$ became totally irreversible, as a consequence of irreversible reactions involving the copper(I) complex and the reduced anthracenyl fragment. For $[CuL^2]^{2+}$, irreversible one-electron oxidative responses were identified at *ca.* +1.0, +1.2 and +1.4 V *vs*. NHE. By comparison, the analogue $[CuL^1]^{2+}$ gave a single broad wave at +1.2 V *vs*. NHE. The unsubstituted $[CuL^3]^{2+}$ yielded a single quasi-reversible wave at *ca.* +1.3 V *vs*. NHE. As this complex has no free amines, this response must be assigned as the $Cu^{III/II}$ couple. Clearly $[CuL^1]^{2+}$ and $[CuL^2]^{2+}$ should also exhibit similar metal-centred oxidations in this region, but their amine oxidation waves fall in the same region so resolution of these various processes is difficult. Nevertheless, it is apparent that metal-centred or amine oxidation in $[CuL^2]^{2+}$ is equally likely, at least from a thermodynamic basis, whereas oxidation of the anthracenyl fragment requires considerably more energy.

Absorption spectroscopy

The solution electronic spectrum of $[CuL^2]^{2+}$ in MeCN exhibits the anticipated d–d maximum at 495 nm, which is comparable with that identified for the analogue $[CuL^1]^{2+}$ (in the same (α) N-based isomeric form).[18] The absorption spectrum measured in water (Fig. 3, inset) exhibited a visible maximum of identical wavelength. The anthracenyl chromophore results in a progression of intense maxima in the near-UV separated by ≈1400 cm^{-1}, representing the aromatic ring breathing vibrational mode in its excited electronic state. The spectrum of the "free" ligand is very similar, except for the absence of the d–d band.

Pulse radiolysis of the copper(II) complexes discussed herein allowed identification of the products of single electron oxidations and reductions in aqueous solution. Oxidation of the parent complex $[CuL^1]^{2+}$ with $^{\bullet}OH$ resulted in the appearance of an intense absorption at *ca.* 400 nm. This spectrum (Fig. 3, solid line) is very similar to that reported for $[CuL^3]^{3+}$ generated by bulk electrolysis of the copper(II) analog in acidic solution, where a prominent maximum at 400 nm was also identified.[19] Similarly, oxidation of the anthracene-substituted macrocycle $[CuL^2]^{2+}$ with $^{\bullet}OH$ gave a spectrum with a prominent maximum around 400 nm (Fig. 3, dotted line). Moreover, there was no change in the anthracene absorption maxima, which indicated that no oxidation of the aromatic group had taken place.

Reduction of $[CuL^2]^{2+}$ with e_{aq}^- gave no significant change in the electronic absorption spectrum, *i.e.* no reduction of the anthracenyl group was evident. A similar observation was made for the reduction of $[CuL^1]^{2+}$. This is indirect evidence for the formation of copper(I) complexes in both cases. The sensitivity of the instrument could not reveal any change in the weak visible d–d maximum of either complex, although this must occur upon reduction of the purple d^9 complexes to the supposedly colourless d^{10} analogues.

Fluorescence spectroscopy

The 298 K fluorescence spectrum of a 10^{-4} mol dm^{-3} MeCN solution of the "free" ligand L^2 (excited at 350 nm) is shown

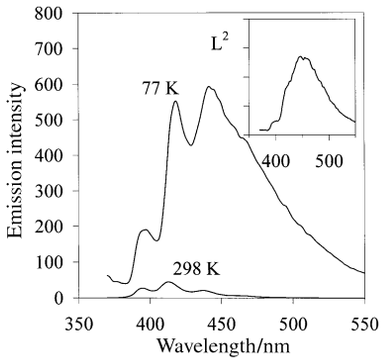

Fig. 4 Luminescence spectra of L^2 (10^{-4} mol dm^{-3} MeCN solution) at room temperature and 77 K (excitation wavelength 350 nm). Inset: 77 K luminescence spectrum at 285 nm excitation.

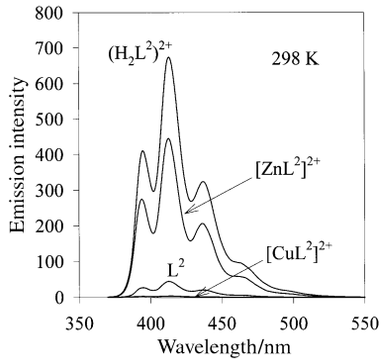

Fig. 5 Room temperature luminescence spectra of $[CuL^2]^{2+}$, L^2, $[ZnL^2]^{2+}$ and $(H_2L^2)^{2+}$. Excitation wavelength 350 nm, 10^{-4} mol dm^{-3} MeCN solutions.

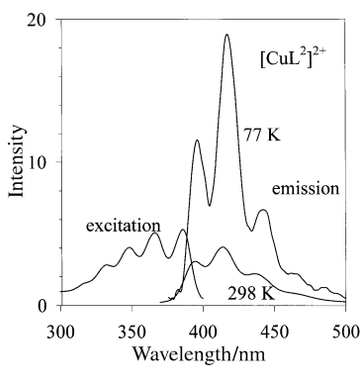

Fig. 6 Luminescence spectra of $[CuL^2]^{2+}$ (10^{-4} mol dm^{-3} MeCN solution) at room temperature and 77 K. Excitation spectrum (420 nm emission) also shown.

in Fig. 4. Weak fluorescence is observed in the room temperature solution spectrum, which increases in intensity by an order of magnitude on cooling to 77 K. A general increase in fluorescence intensity is to be expected on cooling due to a decrease in radiationless relaxation channels. However, the increase observed here is much larger than observed for related compounds such as 9-methylanthracene and we take this behaviour as indicative of room temperature PET.[20] A notable feature in the low temperature spectrum is the appearance of a broad, structureless emission band on the low-energy side of the anticipated vibrational progression. This longer wavelength emitting species can be selectively excited at 285 nm (Fig. 4, inset). The absence of vibrational structure and the red-shift in fluorescence wavelength is consistent with emission from a charge-transfer complex (exciplex).[21] This effect has been seen in a number of other substituted anthracene systems.[22] It appears that, on freezing, a significant proportion of the ligand L^2 is trapped in a conformation where a close interaction between the macrocyclic amines and the anthracene group is achieved, resulting in red-shifted luminescence.

On the basis of the electrochemical measurements, the room temperature PET reaction must involve reductive quenching of the anthracenyl fluorophore by the adjacent free amines, so protonation of the amines should revive fluorescence. Indeed, titration of a solution of L^2 with CF_3CO_2H results in a more than tenfold fluorescence enhancement relative to the room temperature spectrum (Fig. 5), with maximum intensity being obtained after the addition of two equivalents of acid per ligand. This is further evidence that PET between amine lone pairs and the anthracenyl group quenches fluorescence of the free base L^2 at room temperature, *i.e.* protonation of L^2 or freezing the solution switches off PET and revives fluorescence. This behaviour is consistent with PET reactions of simple analogues such as 9-aminomethylanthracene, which also show pH-dependent fluorescent behaviour.[1]

The d^{10} analogue $[ZnL^2]^{2+}$, formed *in situ* by titrating an MeCN solution of L^2 with $Zn(OAc)_2$, fluoresces strongly at room temperature (Fig. 5). This redox inactive complex exhibits no absorption maxima to lower energy of the anthracenyl fluorescence, and so is unable to quench fluorescence by either PET or EET. It also appears that the pendant amines are both co-ordinated in $[ZnL^2]^{2+}$ in a similar fashion to that observed in the crystal structure of the parent hexaamine $[ZnL^1][ClO_4]_2$.[23] Any non-co-ordinated amines in $[ZnL^2]^{2+}$ should quench fluorescence through PET, as seen in the 298 K fluorescence spectrum of L^2.

A 10^{-4} mol dm^{-3} MeCN solution of the complex $[CuL^2][ClO_4]_2$ excited at 350 nm exhibits very weak fluorescence at 298 K (Fig. 6). Addition of successive equivalents of CF_3CO_2H to the solution to generate the protonated complexes $[Cu(HL^2)]^{3+}$ and $[Cu(H_2L^2)]^{4+}$ gave no significant fluorescence enhancement. This is clear evidence that, in contrast to L^2, room temperature fluorescence quenching observed for $[CuL^2]^{2+}$ does not involve PET reactions with the lone pairs of either non-co-ordinated pendant amine. Most importantly, the fluorescence intensity of $[CuL^2]^{2+}$ is also relatively unaffected on cooling to 77 K (fluorescence enhancement of *ca.* 4), compared to the much greater temperature dependent fluorescence of the "free" ligand. This is indicative of (temperature independent) EET[20] between the anthracenyl fluorophore and the metal centre in $[CuL^2]^{2+}$.

Discussion

Depending on the guest ion (or ions) present, various luminescence quenching mechanisms are possible in systems containing the luminophore L^2. Using the electrochemically determined ground state redox potentials for $[CuL^2]^{2+}$ and L^2 and their emission wavelengths, the overall driving force for all possible PET reactions in this system can be estimated,[24] using eqn. (3) where w_p (eV) $= (z_{D^+}z_{A^-})e/4\pi\varepsilon_0\varepsilon_r d_{D-A}$. In this case, the

$$\Delta G_{el}\,(\text{eV}) = E^\circ\,(\text{D}^+\text{–D}) - E^\circ\,(\text{A–A}^-) - \Delta G_{00} + w_p \quad (3)$$

charges ($z_{D^+}z_{A^-}$) on the oxidised (anthracenium cation) and reduced (Cu^+) components are equal, the D–A separation (d_{D-A}) is 6.1 Å from the crystal structure, the relative permittivity of acetonitrile (ε_r) is 37 giving a Coulombic work term (w_p) of 0.064 eV. The redox potentials of the donor and acceptor are +1.9 and −1.05 V *vs.* NHE respectively, the energy of the excited state (≈390 nm) is approximately 3.18 eV, giving an overall free energy change (ΔG_{el}) of −0.17 eV for the intramolecular PET reaction involving oxidative quenching of the anthracenyl group by the metal centre in $[CuL^2]^{2+}$. Alternatively, if the metal centre (E° +1.4 V *vs.* NHE) is oxidised concurrently with reduction of the aromatic group (E° −1.76 V *vs.* NHE), then we calculate an overall free energy change of

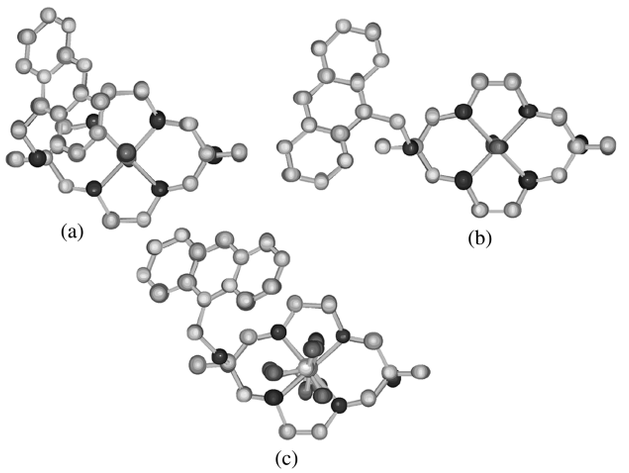

Fig. 7 Molecular mechanics refined structures of $[CuL^2(OH_2)_2]^{2+}$: (a) 68.24 kJ mol^{-1} and (b) 81.16 kJ mol^{-1}. Structure (c) is the strain energy minimised structure of $[CuL^2(OClO_3)_2]$ showing the greater steric effect of the ClO_4^- group.

−0.02 eV. Both PET pathways are associated with rather small free energy changes, and in fact neither can compete with energy transfer from the anthracenyl group to the metal centre. A similar analysis for the observed reductive quenching of L^2 luminescence (in its free base form) is more problematical as calculation of the Coulombic term requires the donor–acceptor distance to be known. The "free" ligand is flexible and it is also not clear which of the six free amines undergoes photoinduced oxidation. If we neglect the Coulombic term, we calculate an approximate driving force of −0.22 eV. Importantly, we note that L^2, like $[ZnL^2]^{2+}$, has no competition from EET deactivation.

More strongly oxidising or reducing metal centres should lead to metal centred PET quenching. Stabilisation of Cu^I may be achieved with S-donor ligands, which has led to oxidative quenching of structurally similar anthracene-substituted ligands.[9] Similarly, trivalent Cu becomes more accessible by complexation with amidate (anionic amide) multidentate ligands and this has resulted in reductive quenching of anthracene fluorescence.[4]

Molecular mechanics modelling of the possible rotational isomers of $[CuL^2(OH_2)_2]^{2+}$ (in the crystallographically observed *trans*-III, α N-based isomer) was performed to investigate the conformational flexibility of the anthracenyl group in solution. First, we note that the lone pair on the anthracenyl-substituted pendant amine points towards the H atoms of the adjacent co-ordinated secondary amines, resulting in significant N···H hydrogen bonds. Therefore, rotation of the C (macrocycle)–N (pendant) bond in either direction would break this hydrogen bond. In addition, steric repulsion between the anthracenyl group and the axially co-ordinated ligands is an important factor. This simplifies the conformational analysis, in that the C (macrocycle)-N (pendant) torsion angle is effectively locked into this position. It emerges that only two of the possible combinations of the N (pendant)-CH_2 and CH_2-C (anthracene) bond torsions lead to stable minima where steric clashing between the anthracenyl group and the macrocycle is avoided. The strain energy minimised structures of these two conformers are shown in Fig. 7. Structure (a) resembles the conformer identified in the crystal structure of the bis-perchlorato complex (see below), and has a calculated strain energy *ca.* 13 kJ mol^{-1} lower than that of conformer (b). Inspection of the relative contributions to the overall strain energies reveals that the higher strain energy of conformer (b) is mainly attributable to more severe H···H non-bonded repulsion. Similar calculations were performed on the bis-perchlorato complex in order to gauge the difference between the solid state and solution structures. The strain energy minimised structure of $[CuL^2(OClO_3)_2]$ (Fig. 7(c)) reproduces the conformation identified in the crystal structure. However, it emerges that anthracenyl group is displaced by *ca.* 1 Å from the metal centre as a result of steric repulsion by the bulky perchlorato ligand compared with that found in the calculated structure of $[CuL^2(OH_2)_2]^{2+}$. This may be an important factor in the solution photochemistry and photophysics of $[CuL^2]^{2+}$.

The spectrofluorometric titration of $[CuL^2]^{2+}$ with acid established an important feature of this system. Protonation of the pendant amines had no effect on fluorescence intensity, which implies that the lone pairs on these amines play no role in the photochemistry of the complex. This is in contrast to studies of other aminomethyl-substituted anthracenes which invariably undergo PET reactions in their free base form, but fluoresce strongly upon protonation. Indeed the "free" ligand L^2 exhibits typical behavior, with fluorescence being revived upon addition of acid. Two factors may contribute to the observed EET behavior of $[CuL^2]^{2+}$. First, the inductive effect of the metal centre should raise the redox potential of the pendant amines, and therefore make an N-oxidative PET reaction unfavourable. As an alternative, or in addition, EET fluorescence quenching of the anthracenyl group by the copper(II) chromophore may simply be more efficient.

Conclusion

We have established that oxidation and reduction of $[CuL^2]^{2+}$ occurs at the metal centre, and the products of these redox reactions have been identified spectrophotometrically. Electrochemistry and fluorescence spectroscopy has shown that the $Cu^{III/II}$ and $Cu^{II/I}$ redox couples of $[CuL^2]^{2+}$ are not accessible in a PET reaction with anthracene as the photoredox active unit. We are currently pursuing other metal centres with a hope to effect photoinduced charge separation. In particular, co-ordination of the anthracene-substituted pendant amine in L^2 may promote electron transfer and we are currently investigating this.

Acknowledgements

Financial support by the Australian Research Council and the Australian Institute for Nuclear Science and Engineering is gratefully acknowledged.

References

1 R. A. Bissell, A. P. de Silva, H. Q. N. Gunaratne, P. L. M. Lynch, G. E. M. Maguire, C. P. McCoy and K. R. A. S. Sandanayake, *Top. Curr. Chem.*, 1993, **168**, 223.
2 A. W. Czarnik, *Acc. Chem. Res.*, 1994, **27**, 302.
3 A. P. de Silva and S. A. de Silva, *J. Chem. Soc., Chem. Commun.*, 1986, 1709.
4 L. Fabbrizzi, M. Licchelli, P. Pallavicini, P. Perotti, A. Taglietti and D. Sacchi, *Chem. Eur. J.*, 1996, **2**, 75.
5 T. D. James, A. S. Sandanayake and S. Shinkai, *Angew. Chem., Int. Ed. Engl.*, 1996, **35**, 1910.
6 C. R. Cooper and T. D. James, *Chem. Commun.*, 1997, 1419.
7 J. Yoon, N. E. Ohler, D. H. Vance, W. D. Aumiller and A. W. Czarnik, *Tetrahedron Lett.*, 1997, **38**, 3845.
8 L. Fabbrizzi, G. Francese, M. Licchelli, A. Perotti and A. Taglietti, *Chem. Commun.*, 1997, 581.
9 G. De Santis, L. Fabbrizzi, M. Licchelli, C. Mangano and D. Sacchi, *Inorg. Chem.*, 1995, **34**, 3581.
10 P. V. Bernhardt, G. A. Lawrance and T. W. Hambley, *J. Chem. Soc., Dalton Trans.*, 1989, 1059.
11 E. Campaigne and W. L. Archer, *J. Am. Chem. Soc.*, 1953, **75**, 989.
12 P. Comba, T. W. Hambley and N. Okon, MOMEC, a molecular mechanics program for co-ordination compounds adapted to HyperChem, Altenholt and Schmitz, Dortmund, 1995.
13 P. V. Bernhardt and P. Comba, *Inorg. Chem.*, 1992, **31**, 2638.
14 S. R. Hall, H. D. Flack and J. M. Stewart (Editors), *The XTAL3.2 User's Manual*, Universities of Western Australia, Geneva and Maryland, 1992.

15 G. M. Sheldrick, *Acta Crystallogr.*, *Sect. A*, 1990, **46**, 467.
16 G. M. Sheldrick, SHELXL 93, Program for Crystal Structure Determination, University of Göttingen, 1993.
17 A. L. Spek, *Acta Crystallogr.*, *Sect. A*, 1990, **46**, C34.
18 P. V. Bernhardt, L. A. Jones and P. C. Sharpe, *J. Chem. Soc.*, *Dalton Trans.*, 1997, 1169.
19 C. Bisi Castellani, L. Fabbrizzi, M. Licchelli, A. Perotti and A. Poggi, *J. Chem. Soc.*, *Chem. Commun.*, 1984, 806.
20 M. R. Wasielewski, G. L. Gaines, M. P. O'Neil, M. P. Niemczyk and W. A. Svec, in *Supramolecular Chemistry*, eds. V. Balzani and L. De Cola, Kluwer Academic Publishers, Dordrecht, 1992, p. 201.
21 G. J. Kavarnos, *Fundamentals of Photoinduced Electron Transfer*, VCH, New York, 1993.
22 J. Dey and I. M. Warner, *J. Phys. Chem. A*, 1997, **101**, 4872 and refs. therein.
23 P. V. Bernhardt, G. A. Lawrance, M. Maeder, M. Rossignoli and T. W. Hambley, *J. Chem. Soc.*, *Dalton Trans.*, 1991, 1167.
24 D. Rehm and A. Weller, *Isr. J. Chem.*, 1970, **8**, 259.

Paper 9/02881A